Computation of the feasible design space for helical extension springs and its parametric representation

Vimalesh Muralidharan

Computation of the feasible design space for helical extension springs and its parametric representation

Vimalesh Muralidharan

Laboratoire des Sciences du Numérique de Nantes (LS2N), CNRS, 44321 Nantes, France {Vimalesh.Muralidharan@ls2n.fr}

Abstract

Springs are commonly used in mechanisms and robotics for imparting stiffness into it or balancing out the gravitational effects. Usually, some kind of design optimization would be performed on the static model of such systems to arrive at a set of suitable spring parameters and its mounting locations. However, in the static model, only the stiffness and free-length parameters of the spring appear explicitly. Thus, only their values would be determined in the design process. But, such a spring may not be practically realizable due to its operation range exceeding the elastic deformation limits or its geometry not satisfying some necessary conditions. Such issues can be avoided only by accounting for the spring design in its entirety (material, geometry, etc.) while designing the mechanical system. This work presents a method that accounts for the above features and derives the complete feasible design space for an extension spring. A parametric representation of this feasible design space has been obtained with two variables. This process has been illustrated for springs mounted on the two sides of a remotely actuated antiparallelogram (X) joint. Finally, a scheme for design optimization of the X-joint considering its geometry, spring, and cable forces, has been proposed using the parametric representation for springs.

Nomenclature

k	spring stiffness/spring rate
d	spring wire diameter
D	spring mean coil diameter
c	spring index (D/d)
N_a	number of active coils in a spring
l_0	free-length of a spring

Continued on the next page

Continued from the previous page

$F^s_{\max}$	maximum force applied on the spring
$l_{\max}$	maximum extension length of a spring
$\delta_{\max}$	maximum deflection in a spring
$\delta^c_{\max}$	maximum deflection in a spring coil ($\delta_{\max}/N_a$)
$\tau_{\max}(d)$	critical shear stress in a spring coil as a function of d
K_w	Wahl's factor to account for the curvature of a spring
ν	factor of safety (1.2)
G_k	shear modulus of the spring material
ρ_k	volumetric density of the spring material
p	pitch of the spring (distance between corresponding points of two successive coils)
ζ	helix angle/pitch angle of the spring
σ_k	parameter $\in [0, 1]$ that maps to the feasible space (d, D) for given k
X-joint	antiparallelogram joint
l	length of the long bars in X-joint
b	length of the short bars in X-joint
$F_{\max}$	maximum force applied by the actuating cables on X-joint
SWFW	stable wrench-feasible workspace

1 Introduction

The schematic diagram of a helical extension spring in its unloaded state is shown in Fig. 1. It is made by winding a steel wire of diameter d around a cylinder successively to form identical coils of nominal diameter D. The coils at the two ends have been bent out as shown in the figure to form hooks on either side of the spring for its attachment. The distance between the inner ends of hooks is the free-length l_0 of the spring. The coils which deform while the spring ends are subjected to a tensile force are referred to as active coils. The number of such coils is denoted by N_a. In the following, details and assumptions on the spring model are stated with justifications.

For an extension spring, the number of active coils is usually assumed to be one less than the total number of coils in the body (N), $N_a = N - 1$ (see e.g., [1], p. 357). The hooks of the spring are designed in several forms depending on the attachment requirements (see e.g., [2], p. 378). In this report, the hooks will be assumed as loops with the same nominal diameter as that of the coil, as depicted in Fig. 1.

These helical springs are found to be manufactured with various carbon steel wires [1]. One of the commonly found materials in the catalog of spring manufacturers is EN 10720-1 (SH/DH)

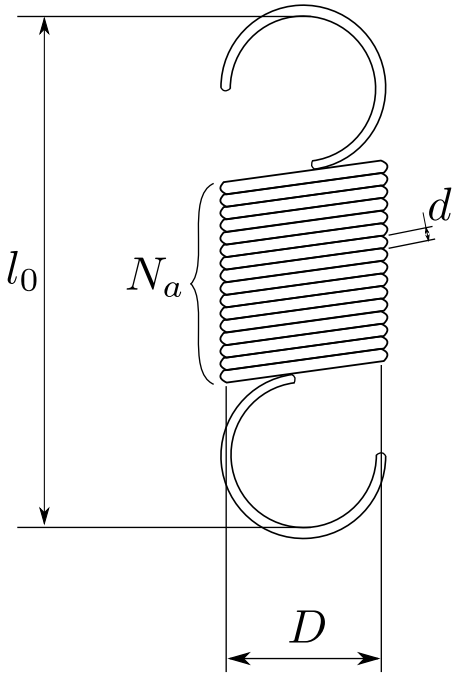

Figure 1: Schematic of a helical extension spring.

(or equivalently ASTM A228), which is also known as the music/piano wire. This material will be assumed for the springs in this report. The mechanical properties of this material can be found in the standard [3]. Notably, the value of shear modulus (G_k) is 81.5 GPa, volumetric density is $\rho_k = 7850$ Kg/m^3. The value of ultimate tensile strength (R_m) varies with the wire diameter (d), as tabulated in [3]. The critical value of shear stress is calculated as $\tau_{\max}(d) = 0.45R_m$ as suggested in [1], p. 348.

The wire diameter (d) is the most influential parameter in spring design, as evident from its exponent in the governing equations (see Eq. (2),(4) in Section 2). Hence, it is customary to use wires of some standard diameters manufactured with a good accuracy. It is possible to find catalogs of spring manufacturers such as Vanel[1], Federnshop[2], where some of these wire diameters are available. Additionally, these manufacturers also permit the user to specify custom parameters (including wire diameter) to fabricate springs with desired properties. For the purpose of this study, the wire diameter (d) is assumed to be a discrete variable that takes the following values $\{0.2, 0.3, \ldots, 6.0\}$ mm.

The force-deflection relationship of an extension spring is modeled as (see [1], p. 355):

$$F = F_0 + k(l - l_0) \tag{1}$$

where F is the tensile force applied on the spring, F_0 its initial tension, k its stiffness, l its deformed length, and l_0 its free-length. In extension springs, initial tension exists a consequence of the twist in the coils that holds them closely together. However, it is said that the initial tension can be

[1]https://www.vanel.com

[2]https://www.federnshop.com

eliminated by using heat treatment methods after fabrication (see [4], p. 6.31). Hence, to simplify this study, initial tension is assumed to be $F_0 = 0$ N.

While an extension spring is loaded in tension, there is shearing load on the coils, torsional load at the interface between hooks and coils, and bending load at the hook (see [1], p.355). However, while designing such a spring, the strength calculations are usually carried out only for the coils (see [1], p. 357), and not the hooks. A recent study [5] has shown that the spring stiffness near its free-length is influenced by the deflection of the hooks. But, in this study, these effects are not considered. They might be a possible extension of this work.

The rest of this report is organized as follows: in Section 2, the governing equations and inequalities of a helical extension spring are presented. In Section 3, springs are designed for a remotely actuated antiparallelogram (X) joint to demonstrate the utility of this work. Finally, the conclusions are presented in Section 4.

2 Governing conditions for spring design

There are two equalities that must be satisfied by a spring. The first one depicts the dependence of the spring stiffness on its geometry and material properties (see [1], p. 355):

$$k = \frac{G_k d^4}{8 N_a D^3} \implies N_a = \frac{G_k d^4}{8 k D^3} \tag{2}$$

The second condition represents the geometric relation between the free-length and other spring parameters, as can be derived from Fig. 1:

$$l_0 = (N_a + 1)d + 2(D - d) \tag{3}$$

Once the material is known a spring is completely defined by the parameters (d, D, k, l_0, N_a). Given that the above two equalities must always be satisfied, it follows that three independent parameters are sufficient to define a spring. A common choice found in the literature [6], [7] is (N_a, d, D). In this report, another set of parameters (k, d, D) will be used to denote a spring design. All the remaining conditions for the feasibility of springs will be derived in terms of these parameters and the feasible spring space will be visualized.

A physically feasible spring must respect the inequality conditions listed below:

- **Strength condition**: The shear stress induced in the spring coils during maximum elongation must be within the elastic limit ($\tau_{\max}$) of the material to ensure its safety. This is given

by (see [1], p. 345):

$$\chi_1 := \tau_{\max}(d) - \nu K_w \frac{8F^s_{\max} D}{\pi d^3} \geq 0, \text{ where} \tag{4}$$

$$\begin{cases} \nu = 1.2 \\ K_w = \frac{4c-1}{4c-4} + \frac{0.615}{c}, \text{with } c = \frac{D}{d} \\ F^s_{\max} = k\delta_{\max} \\ \delta_{\max} = (l_{\max} - l_0) \end{cases} \tag{5}$$

where $\tau_{\max}(d)$ is the limiting shear stress of the material computed from [3] as explained above. A factor of safety $\nu = 1.2$ is considered to ensure safe operation of the spring near its elongation limits. The factor K_w is a function of the spring index $c(= D/d)$, which accounts for the curvature of the spring [8]. The factor $F^s_{\max}$ is the force induced in the spring at its maximum deflection $\delta_{\max}$. The maximum extension length and free-length of the springs are denoted by $l_{\max}, l_0$, respectively. At this stage no information on l_0 or $l_{\max}$ is known. Hence, this condition can be further treated only based on its application and the data (if any) on its attachment points.

- **Number of active coils**: For cold coiled extension springs, the standard [9] specifies the following condition:

$$\chi_2 := N_a - 3 \geq 0 \tag{6}$$

- **Spring index**: The standard [9] specifies the following conditions for the spring index $c(D/d)$:

$$\chi_3 := \begin{cases} c - 4 \geq 0 \\ 20 - c \geq 0 \end{cases} \tag{7}$$

- **Helix angle**: The helix angle of extension spring is defined as (see [10], p. 201):

$$\zeta = \arctan(p/\pi D) \tag{8}$$

where p is the pitch of the spring. At the unstretched configuration (Fig. 1), the pitch $p = d$. The formula presented in Eq. (4) holds exactly only when the helix angle is zero. But, in reality ζ is never exactly zero. Wahl in [8], p.42, notes that Eq. (4) differs from the actual behavior by only less than 2% while the spring index is greater than 3 and ζ is small. Parades in [10], p. 58, presents a limit of 7.5° for ζ to use the above formulation.

The maximum value of ζ occurs while the spring is at its maximum elongation. This value must be smaller than the specified limit:

$$\chi_4 := 7.5^\circ - \zeta_{\max} \geq 0 \tag{9}$$

$$\begin{cases} \zeta_{\max} = \arctan(\frac{d+\delta^c_{\max}}{\pi D}), \text{ where} \\ \delta^c_{\max} = \frac{\delta_{\max}}{N_a} = \frac{(l_{\max} - l_0)}{N_a} \end{cases} \tag{10}$$

Using Eqs. (2),(3), N_a and l_0 can be written in terms of the independent spring parameters (k, d, D). Thus, the conditions in Eqs. (6), (7) can be readily obtained in terms of (k, d, D). If one obtains a value for $l_{\max}$ or formulates it in terms of the other geometric parameters, the inequalities in Eq. (4), (9) can also be written in terms of (k, d, D). In addition to the inequalities $\chi_1, \ldots, \chi_4$, new conditions on spring installations arising from specific applications can also be accommodated, if they could be expressed in terms of the independent spring parameters (k, d, D).

In the following, the above design process is applied to springs in the X-joint.

3 Example: X-joint

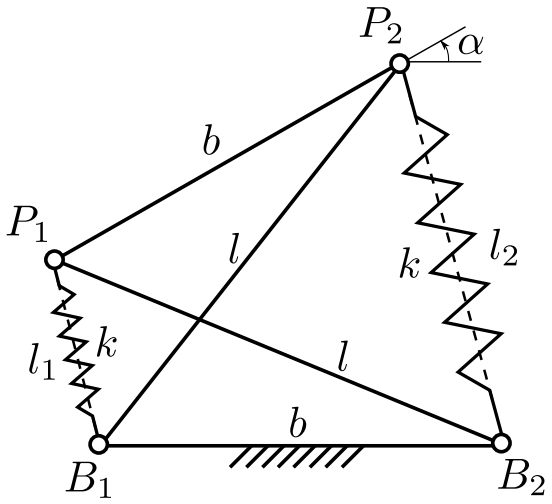

Figure 2: Schematic of X-joint.

The schematic of an antiparallelogram (X) joint is shown in Fig. 2. Among other applications, it has been used to develop robot manipulators inspired from the neck of a bird [11], [12], [13]. It is composed of a base and top bar each of length b and two crossed bars of length l, satisfying the condition $(l > b)$. The orientation of the top bar relative to the base is given by α. The joint is equipped with identical springs on the two sides for imparting stiffness into the system. It is actuated remotely with two cables arranged in parallel with the two springs.

The goal of this study is to find feasible springs for this joint satisfying all the conditions listed in the previous section. In this exercise, the geometry of the joint (b, l) is assumed to be known.

The following constraint is imposed on the outer diameter of the spring to ensure that the joint is compact:

- **Compactness**: The outer diameter $(D + d)$ of the springs is set to be less than one-third of the joint width (b):

$$\chi_5 := \frac{b}{3} - (D + d) \geq 0 \tag{11}$$

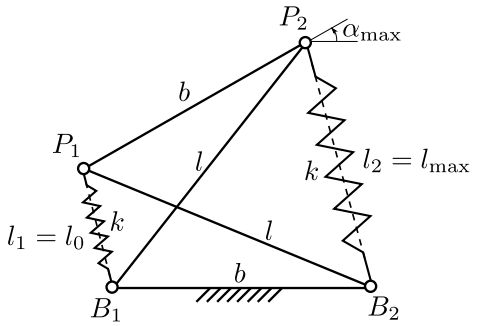

(a) Case A: $(l-b) < l_0 \leq \sqrt{l^2 - b^2}$

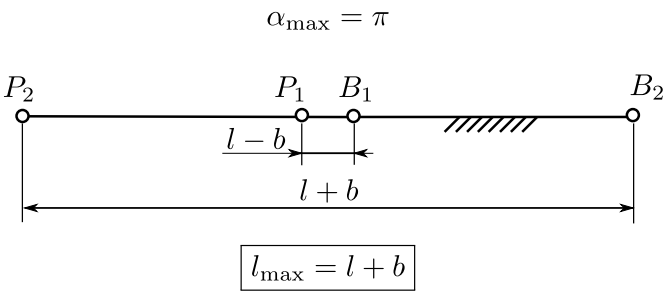

(b) Case B: $0 < l_0 \leq (l-b)$

Figure 3: Two cases based on the free-length l_0 of the installed springs.

The next task is to determine the maximal elongation ($l_{\max}$) required for the springs to be installed in this joint. This information would be useful to evaluate the conditions in Eq. (4) and Eq. (9). Owing to the symmetry of the joint (see Fig. 2), it is apparent that both springs would have the same range of operation. Also, while one spring is at its minimum deployed length, the other one would be at its maximum elongation.

From Fig. 2, it is inferred that the joint range of movement depends on the free-length l_0 of the springs installed. Broadly, this study can be classified into two cases: case A ($l - b < l_0 \leq \sqrt{l^2 - b^2}$) and case B ($0 < l_0 \leq l - b$). In the former, range of movement decreases as l_0 increases and becomes null when $l_0 = \sqrt{l^2 - b^2}$. While in case B, the joint is allowed to execute $\alpha \in]-\pi, \pi[$, irrespective of l_0. These are depicted pictorially in Fig. 3. In each of these cases, different expressions for the maximal elongation would be obtained as explained in the following sections.

3.1 Case A: $(l-b) < l_0 \leq \sqrt{l^2 - b^2}$

Firstly, the inequalities associated with this case are listed:

- **Case A**: Conditions on l_0:

$$\chi_{6a} := \begin{cases} l_0 - (l-b) \geq 0 \\ \sqrt{l^2 - b^2} - l_0 \geq 0 \end{cases} \tag{12}$$

From the geometry of the X-joint (see Fig. 2), it has been shown that: $l_1 l_2 = l^2 - b^2$, throughout the entire range of movement (see e.g., [14], p. 186). Thus, at the limit of α shown in Fig. 3a, the following relation must hold true:

$$l_0 l_{\max} = l^2 - b^2 \implies l_{\max} = \frac{l^2 - b^2}{l_0} \tag{13}$$

Recall that l_0 can be expressed in terms of the independent spring parameters (k, d, D) using Eqs. (2), (3). Thus, from the above condition, $l_{\max}$ can also be obtained in terms of (k, d, D).

3.2 Case B: $0 < l_0 \leq (l - b)$

Considering that $l_0 > 0$ would be satisfied by default (see Eq. (3)), the only inequality representing this case is:

- **Case B**: Condition on l_0:

$$\chi_{6b} := (l - b) - l_0 \geq 0 \tag{14}$$

From Fig. 3b, it is apparent that the maximal spring elongation in this case is given by:

$$l_{\max} = l + b \tag{15}$$

In the following section, all the inequalities derived have been consolidated to construct the feasible spring space.

3.3 Feasible spring space

The set of all the conditions derived for the spring feasibility in Sections 2, 3.1, and 3.2, can be consolidated into two sets, $\boldsymbol{\chi}_a$ and $\boldsymbol{\chi_b}$, based on the two cases A and B, respectively. These are:

$$\boldsymbol{\chi}_a(k,d,D) = \begin{cases} \chi_1 \left(l_{\max} = \frac{l^2-b^2}{l_0}\right) \\ \chi_2 \\ \chi_3 \\ \chi_4 \left(l_{\max} = \frac{l^2-b^2}{l_0}\right) \\ \chi_5 \\ \chi_{6a} \end{cases} \qquad \boldsymbol{\chi}_b(k,d,D) = \begin{cases} \chi_1 \left(l_{\max} = l + b\right) \\ \chi_2 \\ \chi_3 \\ \chi_4 \left(l_{\max} = l + b\right) \\ \chi_5 \\ \chi_{6b} \end{cases} \tag{16}$$

All the feasible spring designs can be obtained by computing the union: $\boldsymbol{\chi}_a \cup \boldsymbol{\chi}_b$. Since all of these conditions have been obtained in terms of (k, d, D), the set of feasible springs can be represented in the design space (k, d, D).

Since the wire diameter d is considered to be a discrete variable (see Section 1), the feasible design space would be a set of 2D (2-dimensional) surfaces in 3D space. However, it would be difficult to represent the same in a figure. Hence, the value of k will be fixed, to visualize the "feasible lines" of d in the (d, D) space. Then, various values of k will be considered to understand the evolution of feasible lines in the (d, D) space.

There are several ways to obtain the feasible lines, the simplest of them being the scanning technique. A more efficient approach would be to rewrite the conditions in Eq. (16) as polynomials in D by suppressing the variable d in the coefficients, and solve the limiting equality conditions to obtain the bounds of D accurately [15]. This process is illustrated for the condition $\chi_1 \left(l_{\max} = \frac{l^2-b^2}{l_0}\right)$ in Appendix A. Other conditions are also treated in the same manner.

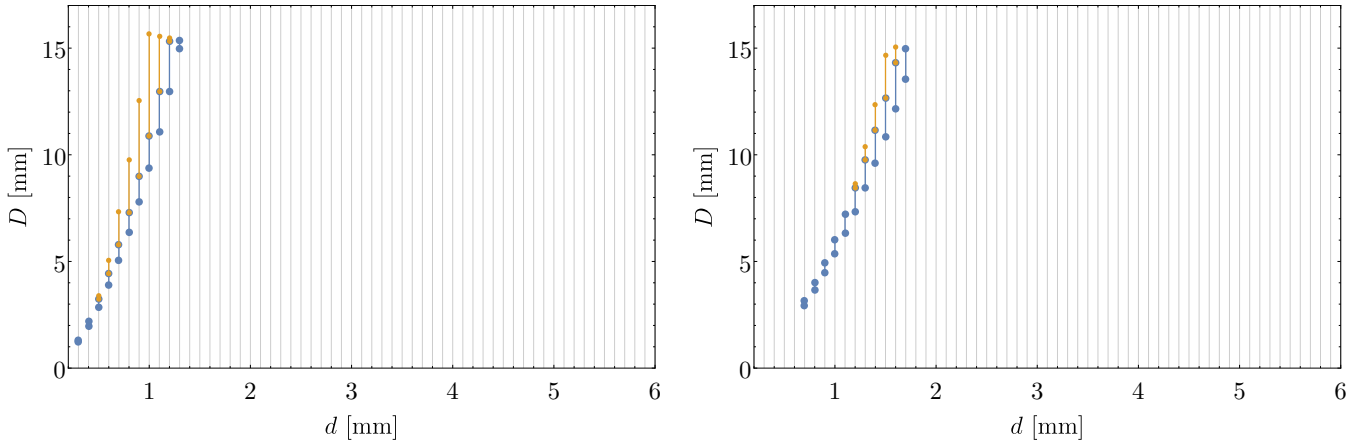

(a) $k = 100$ N/m

(b) $k = 500$ N/m

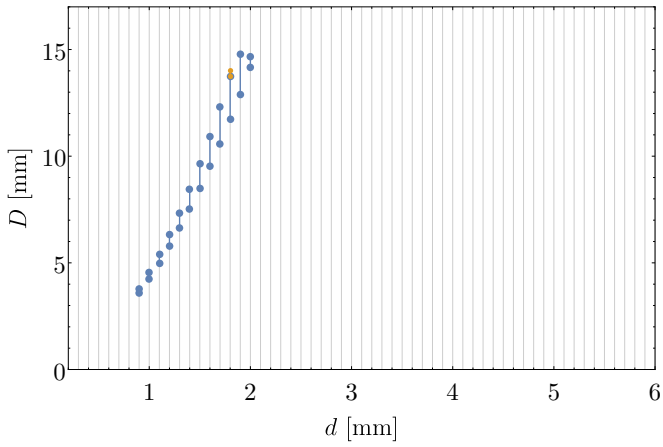

(c) $k = 1000$ N/m

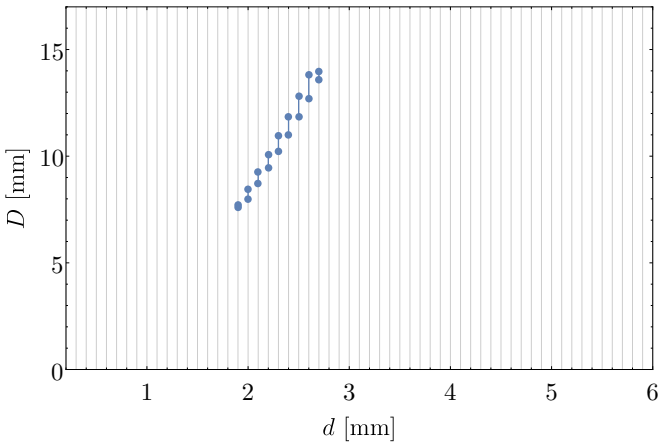

(d) $k = 5000$ N/m

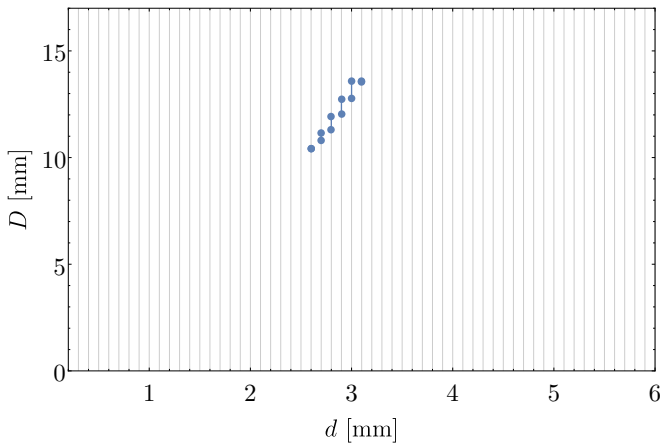

(e) $k = 10000$ N/m

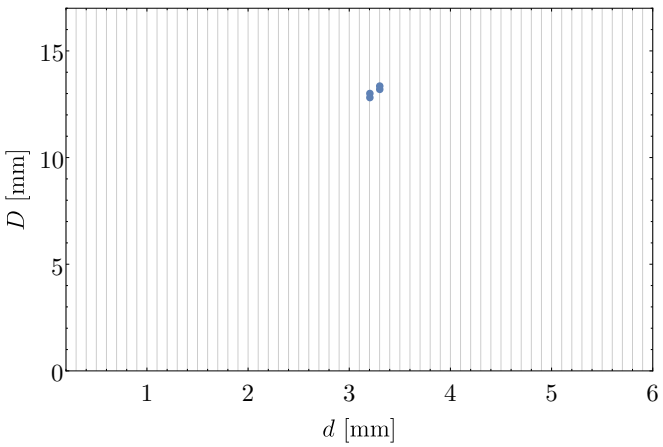

(f) $k = 15000$ N/m

Figure 4: Feasible spring space (d, D) for different values of k. The designs satisfying conditions $\boldsymbol{\chi}_a$ (resp. $\boldsymbol{\chi}_b$) are shown in blue (resp. orange) lines.

As a numerical illustration, consider the X-joint with geometry $b = 0.05$ m, $l = 0.15$ m. The feasible spring space for different values of k are shown in Fig. 4. The designs satisfying $\boldsymbol{\chi}_a$ (resp. $\boldsymbol{\chi}_b$) are shown in blue (resp. orange) lines. Firstly, feasible designs could be found only when $k \in [0.4, 16700]$ N/m, which is a useful information for the designer. In this range, the feasible lines reduce in size and move towards larger d as k increases. It is interesting to note that for $k \geq 1200$ N/m, only designs satisfying $\boldsymbol{\chi}_a$ can be found. This implies that with such strong springs the X-joint cannot exhibit $\alpha \in]-\pi, \pi[$ range of movement.

3.4 Parametric representation and design scheme

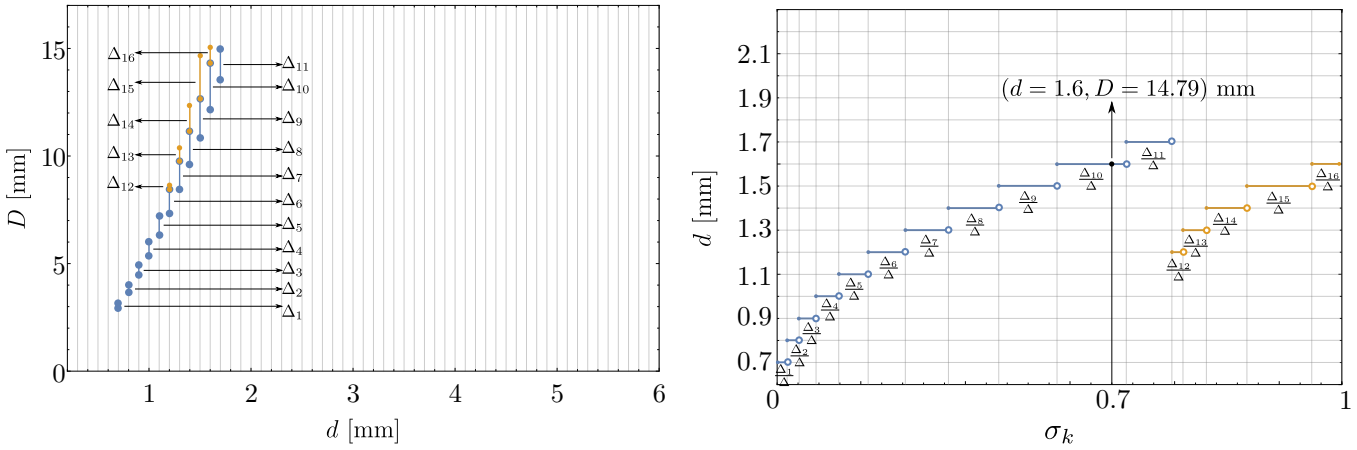

(a) Feasible intervals Δ_i of D in (d, D) space

(b) Mapping the feasible intervals Δ_i to a fraction $\sigma_k \in [0, 1]$

Figure 5: Parametrization of the feasible spring space with $\sigma_k \in [0, 1]$ with $k = 500$ N/m for the X-joint with $b = 0.05$ m, $l = 0.15$ m.

The goal of this section is to propose a parametric representation of the feasible spring space, that can be used for design optimization of the spring in isolation or in combination with its applied mechanical system. From the previous section, it is clear that once k is known, the feasible spring space is formed by a set of line segments in (d, D) space. These segments represent feasible intervals Δ_i of D for the given value of d.

For instance, consider the case when $k = 500$ N/m in Fig. 4. There are 16 feasible intervals of D, $\Delta_1, \ldots, \Delta_{16}$, for different values of d, as shown in Fig. 5a. These intervals can be normalized as $(\frac{\Delta_i}{\Delta})$, where $\Delta = \sum_{i=1}^{16} \Delta_i$. This allows one to arrange them successively as shown in Fig. 5b, thereby creating a map of the normalized intervals to a fraction $\sigma_k \in [0, 1]$ and vice versa. For every value of σ_k in its domain, there exists a point (d, D), which can be back tracked. An illustration with $\sigma_k = 0.7$ as been presented in Fig. 5b. This way the feasible points in (d, D) space can be accessed with a just single parameter σ_k.

It has to be noted that the map from σ_k to the intervals has several discontinuities as seen in

Fig. 5b. In the algorithm, we have arbitrarily assigned the right hand limit for $d(\sigma_k)$, at all such values of σ_k. This leads to the loss of upper bounding point in all the intervals, except the last one, as highlighted in Fig 5b. However, the loss of a few discrete points in an ∞^1 space is an acceptable compromise, considering that we have obtained a one-parameter representation of that space.

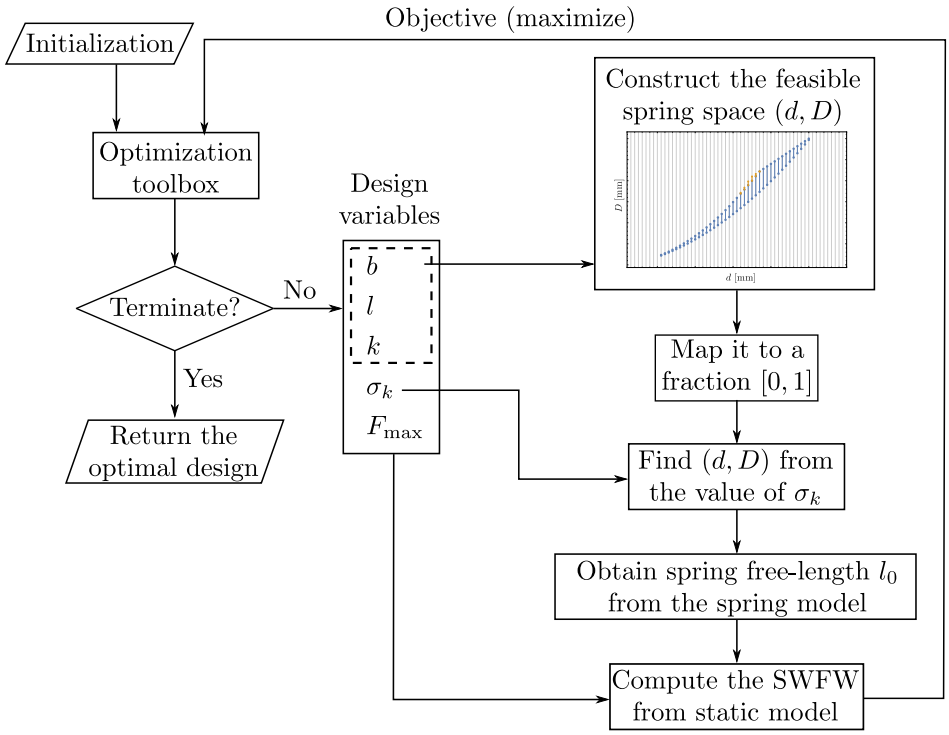

Figure 6: Design scheme for optimizing the geometry, spring, and force variables of X-joint to obtain a maximum SWFW.

In summary, one can use just two parameters (k, σ_k) to access all the feasible spring designs for any given application. This allows the designer to pose a design optimization of the spring, e.g., minimizing its mass/size, as a two-variable problem, instead of a three-variable problem as in [6], [7]. More interestingly, this parametrization allows the designer to integrate the spring parameters (k, σ_k) in the design optimization of its deployed mechanical system, while ensuring its physical feasibility. For instance, the X-joint shown in Fig. 2 can be designed to have a large stable wrench-feasible workspace (SWFW), by considering its geometry, spring, and maximal cable force ($F_{\max}$) as variables. The computational scheme of this process is depicted in Fig. 6.

4 Conclusion

This report has presented a method to compute the complete feasible design space of a helical extension spring. It accounts for the constraints on allowable shear stress, recommended spring index, standard wire diameters, minimum number of active coils, and safe helix angle, for the spring.

Additionally, it also includes the constraints on free-length, maximum extension, and maximum outer diameter of the spring, which are normally obtained from its application.

The spring design space has been visualized in terms of its stiffness (k), wire diameter (d), and mean coil diameter (D). It has been shown that the feasible design space comprises a set of two-dimensional surfaces in (k, d, D) space, which can be parametrized using only two variables (k, σ_k), with $\sigma_k \in [0, 1]$.

As an illustration, the feasible design space and its parametric representation have been presented for the springs mounted on the two sides of an antiparallelogram (X) joint. Finally, a scheme for the optimal design of the X-joint considering its geometry, springs, and actuation forces, has been presented using this parametric representation. In future, this method will be applied to the design optimization of other mechanical systems that use springs.

Appendix A Derivation of polynomial from the condition χ_1

For case A, substituting $l_{\max} = \frac{l^2-b^2}{l_0}$, in χ_1 in Eqs. (4),(5), results in the following limiting equation:

$$\tau_{\max}(d) - \nu K_w \frac{8k(l^2-b^2)D}{\pi l_0 d^3} = 0 \tag{17}$$

Taking common denominator ($\neq 0$) and clearing it:

$$8b^2DkK_w\nu + \pi d^3 l_0 \tau_{\max}(d) - 8DkK_w l^2\nu + 8DkK_w l_0^2\nu = 0 \tag{18}$$

Substituting for l_0 from Eqs. (2),(3), and K_w from Eq. (5), and clearing the common denominator results in the following polynomial:

$$\gamma_0 + \gamma_1 D + \gamma_2 D^2 + \gamma_3 D^3 + \gamma_4 D^4 + \gamma_5 D^5 + \gamma_6 D^6 + \gamma_7 D^7 + \gamma_8 D^8 + \gamma_9 D^9 + \gamma_{10} D^{10} = 0 \tag{19}$$

where

$$\begin{cases} \gamma_0 = -123d^{12}G_k^2\nu \\ \gamma_1 = 73d^{11}G_k^2\nu \\ \gamma_2 = 200d^{10}G_k^2\nu \\ \gamma_3 = 8d^8G_k(246k\nu - 25\pi d\tau_{\max}(d)) \\ \gamma_4 = 8d^7G_k(25\pi d\tau_{\max}(d) - 638k\nu) \\ \gamma_5 = -864d^6G_k k\nu \\ \gamma_6 = -64d^2k\left(123k\nu\left(b^2-l^2\right) - 25d^3(4G_k\nu + \pi\tau_{\max}(d)) + 123d^2k\nu\right) \\ \gamma_7 = 64dk\left(73b^2k\nu - 75\pi d^3\tau_{\max}(d) + 565d^2k\nu - 73kl^2\nu\right) \\ \gamma_8 = 128k\left(100b^2k\nu + 25\pi d^3\tau_{\max}(d) - 292d^2k\nu - 100kl^2\nu\right) \\ \gamma_9 = -32512dk^2\nu \\ \gamma_{10} = 51200k^2\nu \end{cases} \tag{20}$$

For a given value of d, all the coefficients will be known as numbers. The roots of the polynomial in Eq. (19) would contain the limiting values of D associated with χ_1 condition. There might be spurious solutions as well, but they can be eliminated safely by inspecting the intervals on number line of D (see [15]).

References

[1] P. R. N. Childs, Mechanical Design: Theory and Applications, 3rd Edition, Butterworth-Heinemann, 2021. doi:10.1016/B978-0-12-821102-1.00015-9.

[2] D. A. Madsen, D. P. Madsen, Engineering Drawing and Design, 6th Edition, Cengage Learning, 2017.

[3] European Standard, EN 10270-1:2022 - Steel wire for mechanical springs - Part 1: Patented cold drawn unalloyed spring steel wire (2022).

[4] J. E. Shigley, C. R. Mischke, T. H. Brown Jr., Standard handbook of machine design, 3rd Edition, McGraw-Hill Education, 2004.

[5] M. Paredes, T. Stephan, H. Orcière, Enhanced formulae for determining the axial behavior of cylindrical extension springs, Mechanics & Industry 20 (6) (2019) 625. doi:10.1051/meca/2019067.

[6] L. Ciupitu, Optimum design of balancing systems with real springs, in: Modeling and Optimization of the Aerospace, Robotics, Mechatronics, Machines-Tools, Mechanical Engineering and Human Motricity Fields, Vol. 555 of Applied Mechanics and Materials, Trans Tech Publications Ltd, 2014, pp. 593–598.

[7] B. S. Yildiz, Optimal design of automotive suspension springs using differential evolution algorithm, Uludağ Üniversitesi Mühendislik Fakültesi Dergisi 23 (3) (2018) 207–214. doi:10.17482/uumfd.476611.

[8] A. M. Wahl, Mechanical Springs, 1st Edition, Penton Publishing Company, 1944.

[9] European Standard, EN 13906-2:2014 - Cylindrical helical springs made from round wire and bar - Calculation and design - Part 2: Extension springs (2014).

[10] M. Paredes, Développement d'outils d'assistance à la conception optimale des liaisons élastiques par ressorts, Ph.D. thesis, Indian Institute of Science (2001).

[11] B. Fasquelle, P. Khanna, C. Chevallereau, D. Chablat, D. Creusot, S. Jolivet, P. Lemoine, P. Wenger, Identification and control of a 3-X cable-driven manipulator inspired from the bird's neck, Journal of Mechanisms and Robotics 14 (1) (2021) 011005. doi:10.1115/1.4051521.

[12] M. Furet, P. Wenger, Kinetostatic analysis and actuation strategy of a planar tensegrity 2-X manipulator, Journal of Mechanisms and Robotics 11 (6) (2019) 060904. doi:10.1115/1.4044209.

[13] V. Muralidharan, P. Wenger, Optimal design and comparative study of two antagonistically actuated tensegrity joints, Mechanism and Machine Theory 159 (2021) 104249. doi:10.1016/j.mechmachtheory.2021.104249.

[14] R. S. Hartenberg, J. Denavit, Kinematic Synthesis of Linkages, McGraw-Hill Book Company, 1964.

[15] V. Muralidharan, P. Wenger, C. Chevallereau, Computation of stable wrench-feasible workspace of cable driven n-x manipulator, in: Proceedings of the 25ème Congrès Français de Mécanique, Nantes, France, 2022.